Paramagnetic–spin-glass–antiferromagnetic phase transitions in $Cd_{1-x}Mn_xTe$ from specific heat and magnetic susceptibility measurements

R. R. Galazka,* Shoichi Nagata, and P. H. Keesom
Department of Physics, Purdue University, West Lafayette, Indiana 47907
(Received 25 April 1980)

Low-temperature specific heat and low-field magnetic susceptibility were measured in $Cd_{1-x}Mn_xTe$ mixed crystals for $0.002 \leq x \leq 0.70$. Three regions of composition can be distinguished in both experiments. For $x < 0.17$ the crystal is paramagnetic at all temperatures. For $0.17 < x < 0.7$, a spin-glass phase is observed, as evidenced by the characteristic cusp in the susceptibility and a linear temperature dependence of the specific heat in the low-temperature regions. Because the material is an insulator at low temperatures, and the Mn interactions are only antiferromagnetic, we believe that the observed spin-glass phase is produced by the frustration of the lattice. For $x = 0.7$ an antiferromagnetic phase is observed. To understand the experimental behavior of the specific heat and susceptibility as a function of temperature and magnetic field for $0.002 < x < 0.17$, we must assume that the distribution of Mn ions deviates strongly from a random distribution. The number of pairs is more than doubled for $x = 0.05$, and 30% higher for $x = 0.1$, than statistically predicted. The number of larger clusters, like triplets, is also significantly higher. Analysis of the data yielded the value of the exchange integral for the nearest-neighbor interaction to be $J_{NN}/k = -0.55 \pm 0.05$ K. The interaction is stronger within the larger clusters, and is described by a different exchange constant $J'_{NN}/k = -4.3$ K.

I. INTRODUCTION

We first review the physical properties of $Cd_{1-x}Mn_xTe$ mixed crystals on which this investigation was carried out. This ternary compound belongs to a group of materials referred to as "semimagnetic semiconductors," i.e., materials in which one component is an ordinary semiconductor, and the second is a magnetic semiconductor.[1] In this mixed crystal the energy of the half filled $3d$ shell of the Mn^{2+} ion lies below the maximum of the valence band[2] and the first excited d state lies above the minimum of the conduction band. The band structure at the center of the Brillouin zone remains unperturbed by the interaction with the $3d$ electrons. In the absence of magnetic field the $Cd_{1-x}Mn_xTe$ mixed crystals behave like typical semiconductors. However, when magnetic field is present, the thermal average of the component of the spin operator along the field, $\langle S_z \rangle$, is no longer zero. The spin exchange interaction between charge carriers and the $3d$ electrons then becomes important, and several anomalies and new effects are observed.[3–5]

To explain the observed anomalies a theoretical model was proposed,[6] in which the exchange interaction between band electrons and magnetic moments of the paramagnetic ions is taken into account. The parameter $\langle S_z \rangle$, central to the theory, can be obtained by magnetization measurements as a function of temperature and magnetic field.[4] If the magnetic structure of the substance is known, one can also try to formulate the $\langle S_z \rangle$ parameter theoretically.

$Cd_{1-x}Mn_xTe$ mixed crystals can be considered as a diluted magnetic semiconductor with antiferromagnetic interaction. Because of the large energy gap (1.6 eV for CdTe, and increasing with the Mn concentration[7]) the material behaves like an insulator at low temperatures. The Cd^{2+} and Mn^{2+} ions randomly occupy a fcc sublattice. This structure has been theoretically predicted[8–11] to have a spin-glass phase for $x > x_c$, where x_c is the percolation threshold. The appearance of the spin-glass phase is directly related to the frustration of the spins on a lattice which does not allow the simultaneous minimization of all exchange energies.

The existence of a next-nearest-neighbor interaction J_{NNN} between magnetic ions could in principle also be important in this context, since this interaction could cause the system to become a spin-glass due to competing interactions with the nearest neighbor. This situation would occur when J_{NNN} is of opposite sign and sufficiently strong to compete with J_{NN}.[12] However, Brumage *et al.*[13] have shown, on the basis of super exchange path arguments, that in the zinc-blende structure J_{NNN} is much smaller than J_{NN}. Therefore we can expect that in $Cd_{1-x}Mn_xTe$ crystal the frustration mechanism should be responsible for the spin-glass phase. The present measurements of $Cd_{1-x}Mn_xTe$ provide experimental evidence supporting this theoretical model.[14]

We note in passing that the formation of the spin-glass phase due to short-range antiferromagnetic in-

 ©1980 The American Physical Society

teraction in insulators was previously reported for amorphous materials,[15,16] but no experimental evidence was found in single crystals.

The magnetic properties of $Cd_{1-x}Mn_xTe$ have been studied by several authors.[17–19] High-field-susceptibility measurements show a Curie-Weiss behavior at high temperatures, while at low temperatures deviations from a Curie-Weiss law have been observed. A cluster model involving several cluster sizes was proposed[19] on the basis of electron-paramagnetic-resonance and high-field-susceptibility measurements.

The purpose of the present investigation is to establish the magnetic structure of $Cd_{1-x}Mn_xTe$ mixed crystals from specific heat and low-field magnetic susceptibility measurements as a function of magnetic field and temperature. We investigated single crystals of $Cd_{1-x}Mn_xTe$ for $0 \leq x \leq 0.7$, i.e., in the whole region where this material forms a single zinc-blende crystallographic phase.[20,21] Specifically, these measurements allow us to draw several quantitative and qualitative conclusions concerning the magnetic structure, the Debye temperature, and the nuclear magnetic field of $Cd_{1-x}Mn_xTe$.

II. THEORY

$Cd_{1-x}Mn_xTe$ mixed crystals are substitutional solid solutions in which the Mn atoms replace Cd atoms in the fcc sublattice. The distribution of Mn ions in the lattice can either be completely random, or it can deviate from a statistical distribution. In both cases, one can expect not only isolated atoms which do not interact with other Mn atoms (singlets), but also a certain number of pairs, triplets, and larger clusters. The number of different types of clusters depends on the Mn concentration x in the crystal.

In our model we have considered only the nearest-neighbor (NN) interaction between Mn ions since the next-nearest-neighbor interaction is expected to be weak. In addition to isolated ions, the model includes three types of small clusters: pairs, open triangles, and closed triangles.[22] The Heisenberg Hamiltonian in the presence of a magnetic field, and its energy eigenvalues for these clusters, are given in Table I. The energy-level diagram corresponding to this case is shown elsewhere.[23]

The low-temperature specific heat connected with magnetic interactions of paramagnetic ions can be

TABLE I. Hamiltonians and their eigenvalues for various clusters, where $S_1 = S_2 = S_3 = \frac{5}{2}$ and $g = 2$.

Pair (P)	$\mathcal{H} = -2J(\vec{S}_1 \cdot \vec{S}_2) - g\mu_B(S_1^z + S_2^z)H$
	$\vec{S}_1 = \vec{S}_2 \equiv \vec{S}$
	$E(S,m) = -J[S(S+1) - \frac{35}{2}] - g\mu_B mH$
	$0 \leq S \leq 5, \quad \lvert m \rvert \leq S$
Closed triangle (T_c)	$\mathcal{H} = -2J[(\vec{S}_1 \cdot \vec{S}_2) + (\vec{S}_2 \cdot \vec{S}_3) + (\vec{S}_3 \cdot \vec{S}_1)] - g\mu_B(S_1^z + S_2^z + S_3^z)H$
	$\vec{S}_1 + \vec{S}_2 + \vec{S}_3 \equiv \vec{S}, \quad \vec{S}_1 + \vec{S}_3 = \vec{S}_a$
	$E(S,m) = -J[(S(S+1) - \frac{105}{4}] - g\mu_B mH$
	$0 \leq S_a \leq 5, \quad \lvert S_a - \frac{5}{2} \rvert \leq S \leq S_a + \frac{5}{2}, \quad \lvert m \rvert \leq S$
Open triangle (T_o)	$\mathcal{H} = -2J[(\vec{S}_1 \cdot \vec{S}_2) + (\vec{S}_2 \cdot \vec{S}_3)] - g\mu_B(\vec{S}_1^z + \vec{S}_2^z + \vec{S}_3^z)H$
	$\vec{S}_1 + \vec{S}_2 + \vec{S}_3 \equiv \vec{S}, \quad \vec{S}_1 + \vec{S}_3 = \vec{S}_a$
	$E(S,S_a,m) = -J[S(S+1) - S_a(S_a+1) - \frac{35}{4}] - g\mu_B mH$
	$0 \leq S_a \leq 5, \quad \lvert S_a - \frac{5}{2} \rvert \leq S \leq S_a + \frac{5}{2}, \quad \lvert m \rvert \leq S$

written as

$$C = \sum_i a_i C_i = \sum_i a_i \left[d \sum_j E_{j,i}(t)/dT \right] , \quad (1)$$

and the magnetic susceptibility as

$$\chi = \sum_i a_i \chi_i = \sum_i \lim_{H \to 0} \left(\sum_j M_{j,i}/H \right) , \quad (2)$$

where the subscript i identifies different size clusters, and a_i, E_{ji}, and M_{ji} represent the fraction, the energy, and the magnetization corresponding to the different size clusters, respectively. We will show in Sec. IV how these results compare with our experimental measurements for small x.

III. EXPERIMENTAL DETAILS

$Cd_{1-x}Mn_xTe$ single crystals were prepared using a modified Bridgman method at the Institute of Physics of the Polish Academy of Sciences, Warsaw. Composition and homogeneity of the samples were analyzed by density measurements, chemical analysis, electron microprobe analysis, and optical-absorption measurements. The measured composition x agrees with the initial fraction of MnTe within a 2% accuracy. All samples were p-type, with hole concentrations of the order of 10^{16} cm^{-3} at 300 K, which is ascribed to Cd or Mn vacancies. $Cd_xMn_{1-x}Te$ mixed crystals can be obtained up to $x = 0.71$ in the zinc-blende (the same as CdTe) crystallographic structure.[20,21] For $x > 0.71$ a second phase, $MnTe_2$, as well as inclusions of Te, are observed,[21] which makes the material unsuitable for our measurements. MnTe is a typical antiferromagnetic compound crystallizing in a hexagonal NiAs structure,[24] with a Néel temperature of 307 K.[25]

Specific-heat measurements for the samples with compositions $x = 0.002$, 0.01, 0.05, 0.10, 0.20, 0.30, 0.50, 0.70, as well as for CdTe, were performed in the temperature range 0.3–60 K and in magnetic fields $H = 0$, 10, 20, and 28 kG. A standard heat-pulse technique was used.[26]

Magnetic susceptibility was obtained by magnetization measurements as a function of temperature in the range 1.1–100 K. A superconducting quantum interference device (rf SQUID) was used to measure the magnetization.[27] Investigations were performed for samples with composition $x = 0.10$, 0.20, 0.30, 0.40, 0.50, 0.60, and 0.70. During the measurements a magnetic field of 15 G was applied. Samples were cooled either in zero field (less than 0.05 G) or in the presence of the 15-G field.

IV. SPECIFIC HEAT

The experimental specific heat (C) results can be divided into two parts. A low-temperature region (below 4 K), where the specific heat is attributed mainly to the Mn ions, and the region $T > 4$ K, where the lattice contribution dominates all other effects.

Figure 1 summarizes the experimental results of the specific heat at $H = 0$ for all measured samples. For $x = 0.002$ the zero-field C is very close to that for CdTe and therefore only the results for 28 kG are plotted for this sample. If we consider the value of C at 1 K as a function of x, it is an increasing function of x up to $x = 0.10$, where the specific heat begins to decrease with increasing x. The influence of magnetic field on C is very significant for samples with $x = 0.002$, 0.01, 0.05, and 0.10, but only a small influence of H on the specific heat was observed for $x = 0.20$, 0.30, and no effect of magnetic field was detected for $x = 0.50$ and 0.70 up to 28 kG. This behavior indicates an increasing degree of clustering of Mn atoms with increasing x. The interaction of these atoms in large clusters exceeds $4k$ (where k is the Boltzmann constant) and the contribution of these clusters to the specific heat below 4 K tends to go to zero.

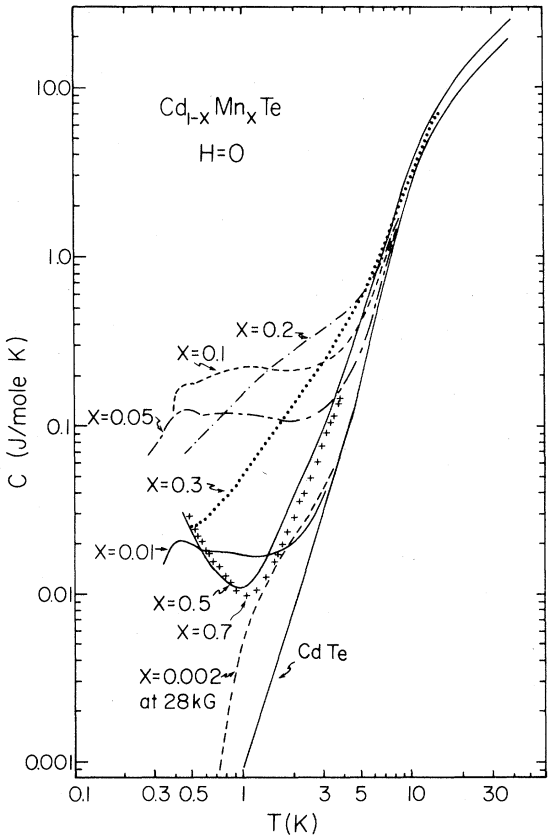

FIG. 1. Specific heat vs temperature for $Cd_{1-x}Mn_xTe$ mixed crystals. For sample $x = 0.002$, the data at zero field are very close to the CdTe specific heat. For this reason only the data for 28 kG are plotted.

The lattice specific heat appears to be a weak function of composition. The high-temperature results are x dependent, the largest value of C corresponding to $x = 0.50$. One can expect changes of the acoustical-phonon spectrum in so wide a range of composition. While the magnetic specific heat can also contribute in the high-temperature region, its value is expected to be small compared to the lattice specific heat.

A. Lattice specific heat

The specific heat in CdTe shows a typical behavior. The Debye temperature Θ_D, defined for six degrees of freedom per molecule as a function of T, is presented in Fig. 2. For $Cd_{1-x}Mn_xTe$ mixed crystals it is impossible to obtain the Debye temperature as T approaches 0 because of the strong influence of magnetic effects. But between 8 and 11 K, where the Debye temperature goes through a minimum for CdTe as well as for the mixed crystals, the lattice contribution is dominant. The Debye temperature was calculated for this region of temperature, and is shown in Table II. Although the Debye temperature varies with composition, the changes are small. Taking into account the possible error connected with the influence of the magnetic contribution to the specific heat at high temperature, our data suggest that the acoustical-phonon spectrum does not change significantly with composition. Previously reported specific heat measurements[28] in CdTe performed for temperatures ranging from 3 to 300 K, agree with our experimental data. From extrapolation of experimental results below 1 K, we also obtain a value for $\Theta_D(T \rightarrow 0) = 158$ K.

B. Magnetic specific heat

From the specific heat results we find that the number of Mn atoms frozen in large clusters increases with the crystal composition x. For samples with $x < 0.10$, in the region in which only small clusters should be important, we can compare our experimental results for C with the theoretical predictions of Eq. (1). We calculated the contributions from

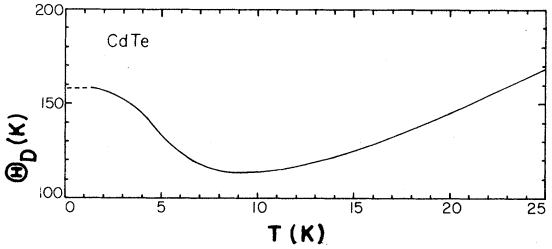

FIG. 2. Debye temperature of CdTe in the low-temperature region.

TABLE II. Debye temperature vs composition of $Cd_{1-x}Mn_xTe$ in the region 9–10 K.

x	0.00 (CdTe)	0.05	0.10	0.20	0.30	0.50	0.70
Θ_D (K)	113	113	110	109	106	106	112

singlets, pairs, and triad clusters to this specific heat. Since these results are applicable only to samples of relatively low values of x, we compare them only with our results for samples with composition $x = 0.002$, 0.01, 0.05, and 0.10. For these samples, we extracted the excess magnetic contribution to C by subtracting the experimental specific heat of CdTe according to $C_{ex} = C - C_{CdTe}$. This procedure is well justified in the low-temperature region $T < 2$ K, where the lattice contribution is at least an order of magnitude smaller than the magnetic specific heat. The error in the value of C_{ex} increases with temperature because the lattice specific heat of these mixed crystals increases very rapidly. In addition, a small error can arise from the fact that the lattice contribution for the mixed crystals probably differs slightly from that for CdTe.

Figure 3 shows the experimental results of the excess specific heat for $x = 0.002$ for three magnetic fields. The theoretical curves for 20 and 28 kG were calculated assuming a statistical distribution of Mn

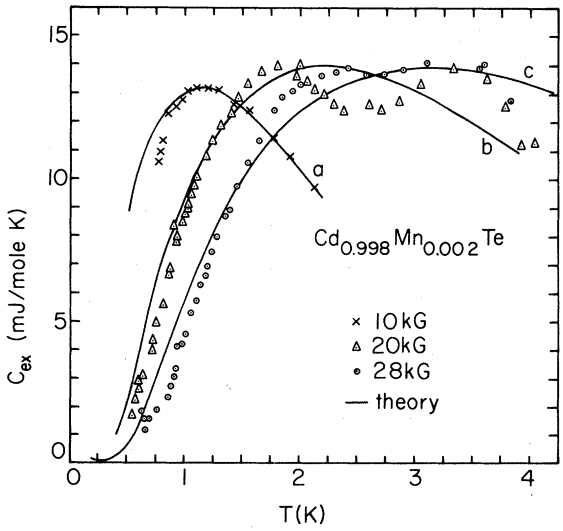

FIG. 3. Excess specific heat (magnetic) for $x = 0.002$ vs temperature. Curve a is calculated assuming a concentration of singlets which is lower by 5% than statistically predicted. Curves b and c are calculated for a statistical distribution of singlets and pairs.

atoms in a fcc sublattice. For 10 kG we had to assume that the number of singlets is 5% smaller than statistically predicted. The values of experimental and theoretical specific heat, as well as the positions of the maxima, are in reasonable agreement. Figure 4 presents the results for the excess specific heat for a sample with $x = 0.05$. Curve a was calculated for $H = 0$ assuming a statistical distribution of pairs, closed triangles, and open triangles (note that in zero magnetic field the contribution of singlets is zero). The values of the parameters used in the calculations are given in Table III. As can be seen, the experimental values are approximately twice as large, and the shape of the theoretical curves do not correspond to the experimental results. It is evident that the number of clusters for $x = 0.05$ is much larger than statistically predicted. In addition, the whole shape of the experimental curve as a function of temperature, as well as the relative peak at 0.4 K, is very characteristic for the pair specific heat. Curve b was calculated by adjusting the number of pairs and assuming the exchange constant $J_{NN}/k = -0.5$ K for best fit to the zero-field data. The fit to the experimental results is very good especially in the low-temperature region. In this calculation we neglected clusters other than pairs. Including such larger clusters does not reproduce the observed peak and does not lead to the observed temperature behavior of C. In the remaining calculations shown in Fig. 4, the number of pairs was assumed to be the same as in curve b. Curve f represents the calculations where the number of singlets was assumed to correspond to a statistical distribution in a magnetic field $H = 28$ kG. It is clear from this curve that the number of singlets must be reduced to obtain agreement with experimental data. Curves c, d, and e were calculated using adjustable values for the number of singlets and keeping the number of pairs and the J_{NN} value constant. It is interesting to note that the number of singlets increases with increasing magnetic field (Table III). For $x = 0.002$ this effect is in the range of error (the difference between the 10 and the 20, 28 kG data), but for $x = 0.05$ and 0.10 it is more significant.

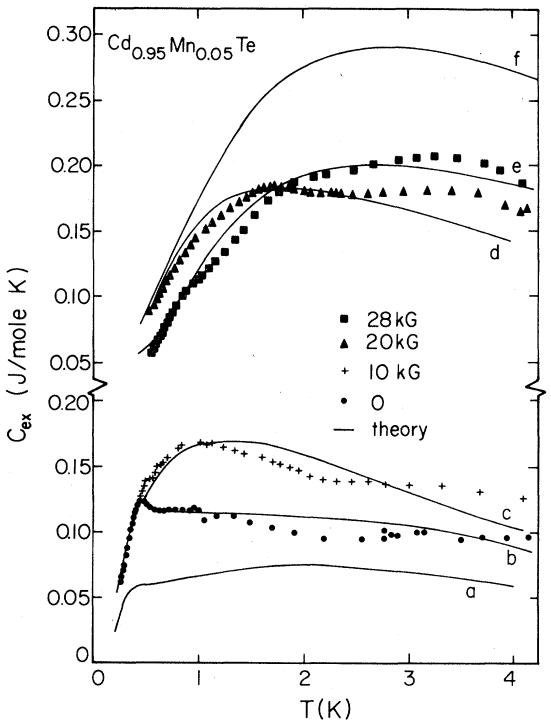

FIG. 4. Excess specific heat (magnetic) for $x = 0.05$ vs temperature. Curve a is calculated assuming statistical distribution of pairs and open and closed triangles at $H = 0$. Curve b is calculated using only pairs, and adjusting their number. Curves c, d, and e are obtained by fitting the number of singlets, and taking the number of pairs established for curve b. Curve f represents the calculated specific heat assuming the same number of pairs as for curve b and a statistical number of singlets. Numerical values are given in Table III.

Our data consistently suggest that the number of singlets N_S is related in some way to the energy of the applied magnetic field. Fitting the data for both $x = 0.05$ and 0.10 shows that N_S is proportional to H^2 (see Table III). In order to understand this phenomenon we have to assume that some small fraction of

TABLE III. Distribution of Mn ions in different clusters vs composition of $Cd_{1-x}Mn_xTe$ in the paramagnetic region.

	at.% of Mn atoms in Singlets in H (kG)					
x	10	20	28	Pairs	Open triangles	Closed triangles
0.002	92.6	97.5	97.5	0.56	0	0
0.05	18.0	22.0	27.6	54.4	0	0
0.10	1.8	4.7	8.5	25.2	14.5	13.2

the Mn ions are only weakly bound to larger clusters. The applied magnetic field effectively frees these spins, which then contribute as additional singlets.

Results of the specific heat measurements on the $x = 0.01$ sample shown in Fig. 5 are qualitatively similar to the results obtained for $x = 0.05$, although we have some difficulty in explaining the quantitative behavior of the specific heat measurements.

The low-temperature specific heat for $T < 0.8$ K measured in zero magnetic field as well as in 20 and 28 kG indicates a large number of pairs: About 30 to 40% of Mn atoms appear to be paired (see Fig. 5, curve a). However, the values of the maxima in the specific heat measured in 20 and 28 kG corresponds to almost 100% of singlets (Fig. 5, curve b). Also the peak of C observed at $T = 0.42$ K in zero magnetic field is sharper than for $x = 0.05$ and the specific heat decreases faster for $T > 0.6$ K than was observed for the $x = 0.05$ sample. Similar behavior was noticed in $Hg_{1-x}Mn_xTe$ for $x = 0.027$.[23] It would appear then that the number of singlets and pairs is a function of temperature. This effect is weak in the case of the $x = 0.05$ sample (see the deviation from the theoretical curve, especially for zero field, in Fig. 4), but is very pronounced for $x = 0.01$.

It is possible that the distance between two-nearest Mn atoms changes with temperature due to a Jahn-Teller effect. If this distance increases with temperature, it will cause a rapid decrease of the value of J_{NN} and a subsequent dissolution of pairs.

In spite of these uncertainties, the $x = 0.01$ sample shows a larger number of pairs at very low temperature than is statistically predicted, and the specific-heat maxima appear at the same temperature as for $x = 0.05$, indicating that the exchange constant J_{NN} is the same for both compositions.

Figure 6 shows results for the $x = 0.10$ sample. The bottom curve is calculated for a statistical distribution of pairs and both types of triangles. We fitted the number of pairs and triangles to obtain the best agreement to experimental data at $H = 0$ and, as before, adjusted the number of singlets at 20 and 28 kG. We were not able to obtain a good agreement within the framework of this simple model. For the $x = 0.10$ sample the fit is worse than for previous samples. Clearly the role of larger clusters, neglected in our calculations, is now also more important. The exchange constant was found to be $J_{NN}/k = -0.6$ K for this composition.

Figure 7 shows the statistical distribution of Mn atoms in singlets and pairs; the indicated points are obtained by fitting the experimental data. Qualita-

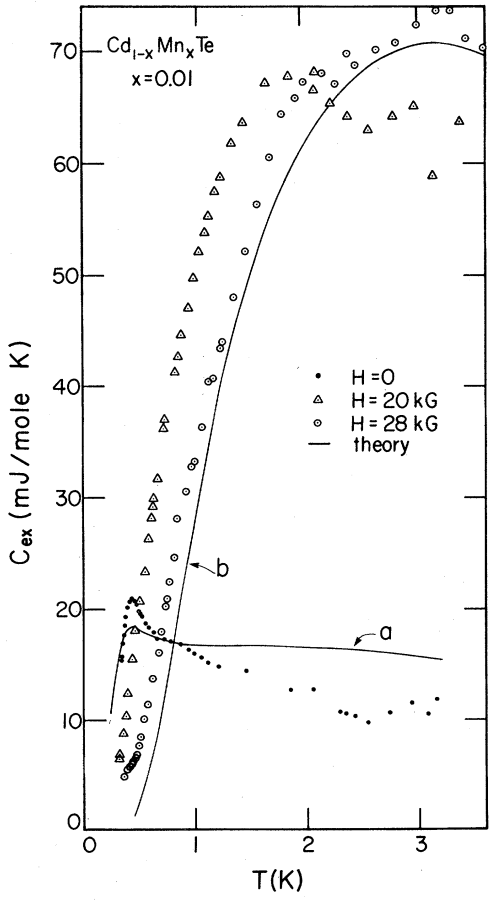

FIG. 5. Excess specific heat (magnetic) vs temperature for $x = 0.01$. Curve a is calculated assuming 40% of the atoms in pairs. Curve b shows the specific heat calculated when 100% of the Mn atoms are singlets in 28 kG.

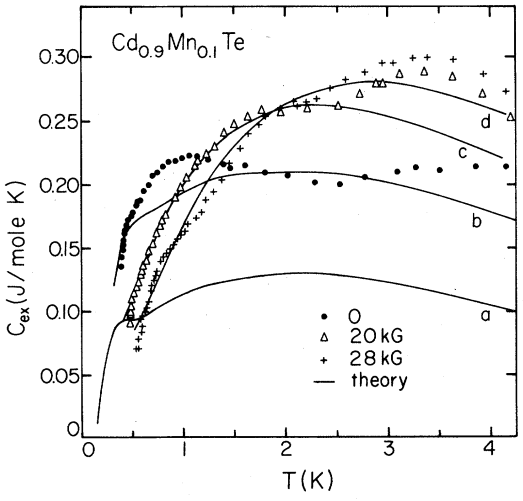

FIG. 6. Excess specific heat (magnetic) vs temperature for $x = 0.10$. Curve a is calculated assuming a statistical distribution of pairs and open and closed triangles at $H = 0$. Curve b is calculated for the fitted number of pairs and triangles. For curves c and d the fitting parameter is the number of singlets (for numerical values see Table III).

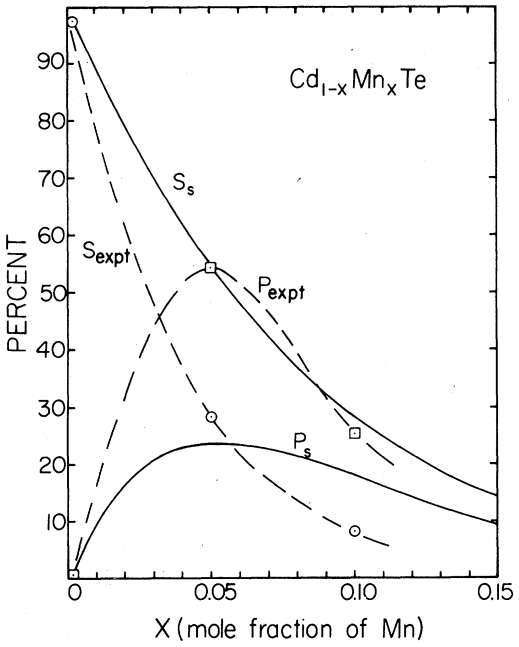

FIG. 7. Statistical and experimentally obtained distributions of Mn ions in singlets and pairs in $Cd_{1-x}Mn_xTe$ (S_s, S_{expt} and P_s, P_{expt}, respectively). The number of pairs can be obtained by dividing curves P_s and P_{expt} by 2.

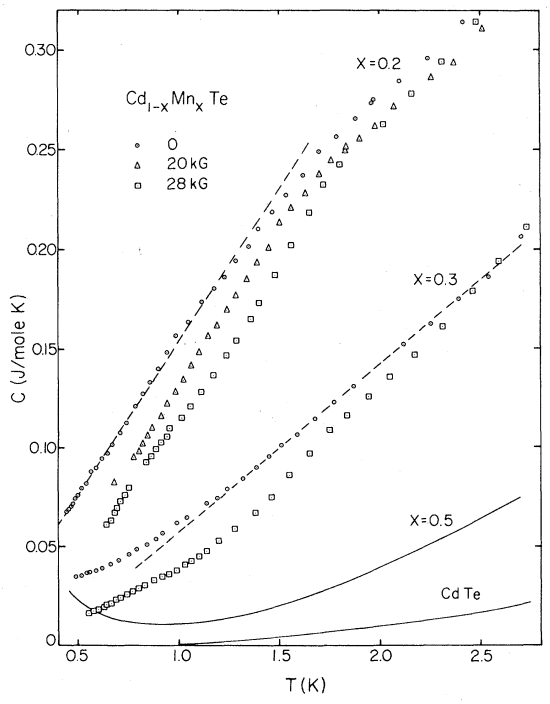

FIG. 8. Low-temperature specific heat for $x = 0.2$, 0.3, and 0.5. Dashed lines show the linear behavior of C vs T for $x = 0.2$ and 0.3.

tively, the distribution obtained is similar to a statistical one. Quantitatively, the deviation from the statistical prediction is very pronounced: the number of singlets and pairs above $x = 0.05$ decreases faster with Mn concentration than statistically predicted. For sufficiently high values of x one thus expects a small number of very large clusters or one infinite cluster.

Figure 8 shows experimental results for C for $x = 0.20$, 0.30, 0.50, and for a CdTe sample in the low-temperature range. Weak magnetic field dependence was observed for samples with $x = 0.20$ and 0.30. No influence of magnetic field was seen for the $x = 0.50$ and 0.70 samples. The linear dependence of C as a function of T in this region of temperature was observed for $x = 0.20$ and 0.30. Similar behavior has been observed previously in metallic spin-glasses such as *Cu*Mn and *Au*Fe,[27,29,30] where magnetic-susceptibility measurements confirmed the idea of the formation of the spin-glass phase.

C. Nuclear specific heat and the antiferromagnetic phase transition

Two samples with the highest Mn concentration $x = 0.5$ and 0.7 differ noticeably from the other measured samples. The specific heat does not depend on magnetic field up to 28 kG, and at the lowest temperatures increases for these samples. For $T < 0.7$ K, specific heat in both samples is proportional to T^{-2}. Such behavior, together with the absence of magnetic field dependence, is typical for nuclear specific heat.[31] The magnetic field which splits the nuclear-spin levels is produced by $3d$ electrons and transferred to the nuclei by the polarization of $1s$ electrons. The average value of the product $C_{Mn}T^2 = 12.4$ mJ K/mole (Mn) is larger than for Mn metal[32] and smaller than the values observed for other insulators containing Mn (such as $KMnF_3$ or $RbMnF_3$).[33] Knowing the nuclear magnetic moment of Mn from NMR experiments, we calculated the strength of magnetic field at the Mn nuclei to be $H = 391$ kG $\pm 5\%$. For both samples this magnetic field is the same within the accuracy given above.

At higher temperatures the specific heat increases. For $x = 0.05$ in the region 0.4 to 2 K, it can be described by the equation $C = 5.77T^{-2} + 5.0T^3$ mJ/mole K. In the region 3 to 10 K the specific-heat C is also proportional to T^3 but with a different coefficient: $C = 3.26T^3$ mJ/mole K. The latter cubic term is connected with the lattice specific heat and corresponds to a Debye temperature of 106 K. It is possible that the low-temperature cubic term contains an additional contribution from spin waves, similar to that observed in $KMnF_3$ and $RbMnF_3$.[33]

Figure 9 shows the high-temperature specific heat for $x = 0.50$, 0.70, and for CdTe, as well as $\Delta C = C_{0.7} - C_{CdTe}$, as a function of temperature. For the $x = 0.70$ sample, C is the same as for CdTe

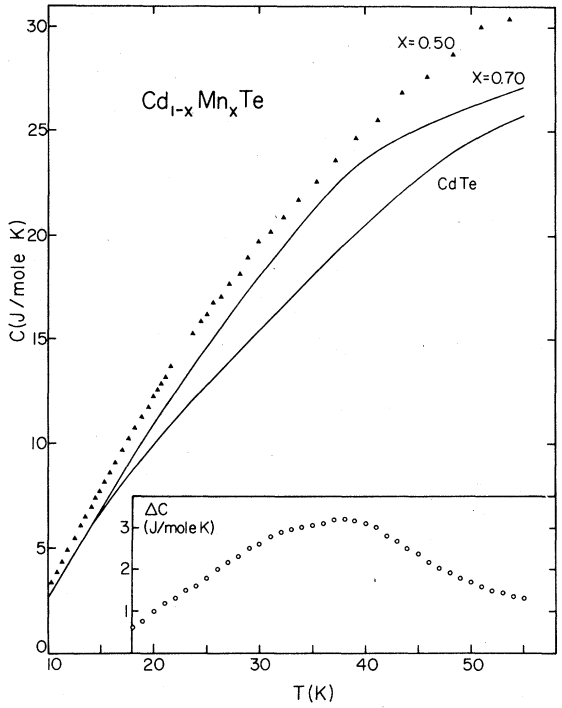

FIG. 9. High-temperature specific heat vs temperature for $x = 0.5$, 0.7, and for CdTe. In the inset, $\Delta C = C_{0.7} - C_{CdTe}$ is plotted.

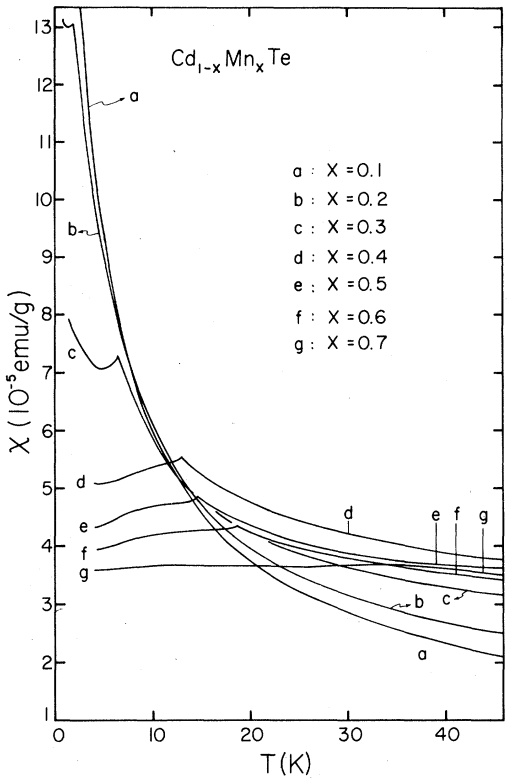

FIG. 10. Zero-field-cooled magnetic susceptibilities of $Cd_{1-x}Mn_xTe$ as a function of temperature for various Mn concentrations x. The relative values are very accurate but the absolute values may contain considerable error.

between 10 and 15 K; the difference, ΔC, increases up to about 40 K, and subsequently decreases. The increment ΔC shows a broad maximum which is probably related to the antiferromagnetic-paramagnetic phase transition, which would agree with the results of magnetic susceptibility measurements. The Néel temperature derived from both experiments equals $T_N = 36 \pm 2$ K.

V. MAGNETIC SUSCEPTIBILITY

Magnetic susceptibility as a function of temperature was investigated by means of magnetization measurements using a SQUID technique. The value of the dc susceptibility $\chi = M/H$ was markedly dependent on the past magnetic history for several of the samples, i.e., whether the specimen had been cooled in the presence or in the absence of an applied magnetic field. For the latter case, the samples were first cooled in a magnetic field of less than 0.05 G and then a magnetic field of 15 G was applied. Cusplike peaks in χ vs T are observed (see Fig. 10) at the temperature T_g for compositions $0.2 \leq x \leq 0.6$. The field-cooled susceptibilities, i.e., when the magnetic field had been applied before the samples were cooled below T_g, are shown in Fig. 11, indicated by primed letters. In this case the susceptibility does now show a cusp at T_g, but remains essentially constant below this temperature. Within spans of 30 min no time dependence of the magnetization could be detected for the field-cooled and zero-field-cooled susceptibilities. The general behavior is identical to that of the metallic spin-glasses CuMn (Ref. 29) and AuFe.[34]

At temperatures well below T_g the susceptibilities increase again, which probably originates from contributions of finite clusters, e.g., single ions, pairs, triplets, etc. For $x = 0.1$ and 0.7 the zero-field-cooled susceptibilities were identical, which suggests that irreversible effects are absent. These experimental results indicate three different magnetic phases, which is consistent with the specific heat measurements. In Fig. 12 is presented a phase diagram for the magnetic properties of the $Cd_{1-x}Mn_xTe$, which is qualitatively in agreement with the theoretical prediction of De Seze.[8] This diagram cannot be extended above $x = 0.71$, since no single crystallographic phase of $Cd_{1-x}Mn_xTe$ could be made for that range.

The low-temperature extension of the boundary between paramagnetic and spin-glass phases gives x_c between 0.1 and 0.2, which is consistent with the

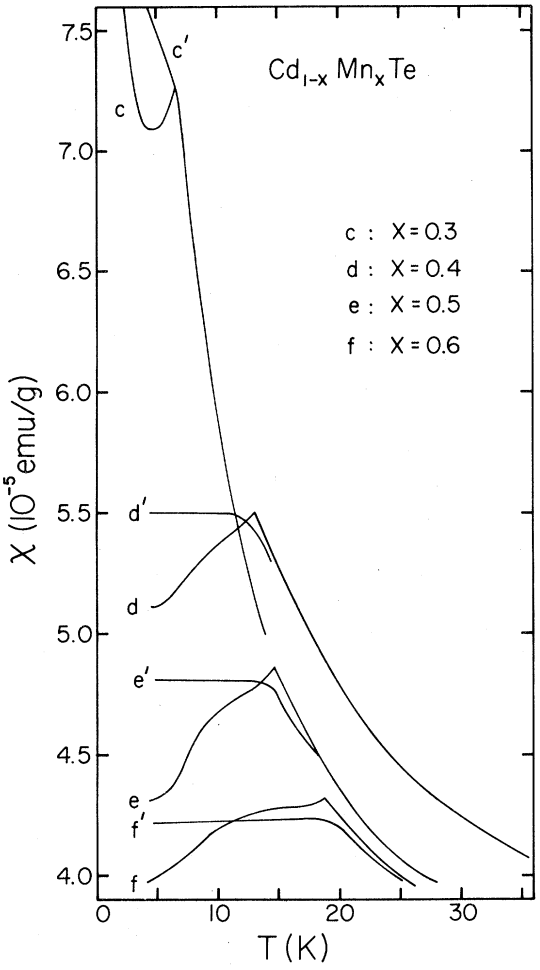

FIG. 11. Magnetic susceptibilities for the spin-glass region of x. Curves marked by unprimed letters correspond to zero-field-cooled susceptibility, and primed letters indicate results for the field-cooled susceptibility (see text).

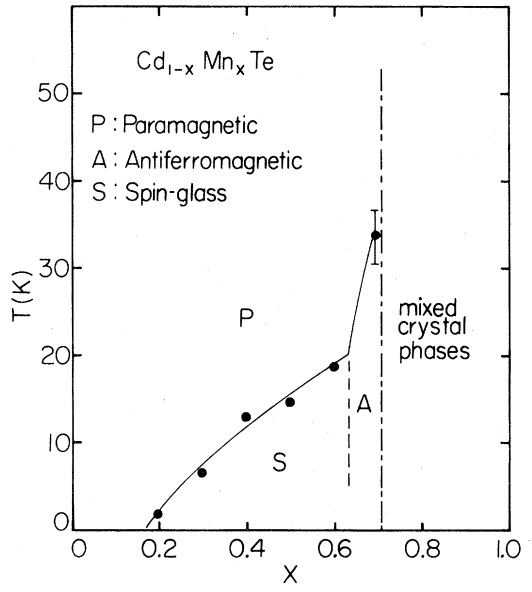

FIG. 12. Phase diagram for temperature vs composition for the magnetic structure of $Cd_{1-x}Mn_xTe$. Regions of P, A, and S indicate paramagnetic, antiferromagnetic, and spin-glass phases, respectively.

simplest estimate of the percolation threshold value for a fcc lattice: $x_c = 0.17$. The system remains paramagnetic for $x < x_c$ for all temperatures, since only finite clusters of antiferromagnetically coupled spins are present. For $x > x_c$ an infinite cluster (or a set of very large clusters) is responsible for the transition into the spin-glass phase.[11] For x between 0.6 and 0.7, there exists a phase boundary between the spin-glass and antiferromagnetic phases. The susceptibility for $x = 0.7$ is independent of temperature below the Néel temperature and is characteristic of a typical antiferromagnetic with a low anisotropy field. The $Cd_{1-x}Mn_xTe$ system becomes antiferromagnetic at low temperatures for $x > 0.6$, but antiferromagnetism appears to be unstable for $x \leq 0.6$.

An approximate value of the exchange constant, $J'_{NN}/k = -4.3$ K, was obtained from the constant value of the susceptibility for $x = 0.7$ using the molecular-field-theory expression, $\chi = N(g\mu_B)^2/4zxJ'_{NN}$, where $g = 2$, N is the number of magnetic ions, z is the number of nearest neighbors, μ_B is the Bohr magneton, and x is the concentration. The value of the exchange constant J'_{NN} differs from $J_{NN}/k = -0.55$ K obtained from low-temperature specific-heat data, and has a different meaning. This J'_{NN} represents the average strength of the exchange interactions present in large clusters (or in an infinite cluster), whereas J_{NN} is connected with exchange interaction between the nearest neighbors in small noninteracting clusters, such as pairs or triplets.

Figure 13 shows the reciprocal susceptibility as a function of temperature for $x = 0.05$ and 0.10 samples. Experimental points are taken from published results.[19] Theoretical curves are calculated assuming the distribution of different clusters derived from specific heat measurements (Table III) and using the exchange constant $J_{NN}/k = -0.55$ K. The number of singlets is assumed to be the same as obtained from specific heat measurements in 10 kG. At high temperatures the theoretical susceptibility is lower than the experimental value, and the difference is larger for the $x = 0.10$ sample.

The difference between experimental results and theoretical calculations result from the inadequacy of our theoretical model. Neglecting clusters larger than triplets, our model in effect neglects about 20% of the ions for the $x = 0.05$ sample and about 50% of Mn ions for the $x = 0.10$ sample. Consequently, the

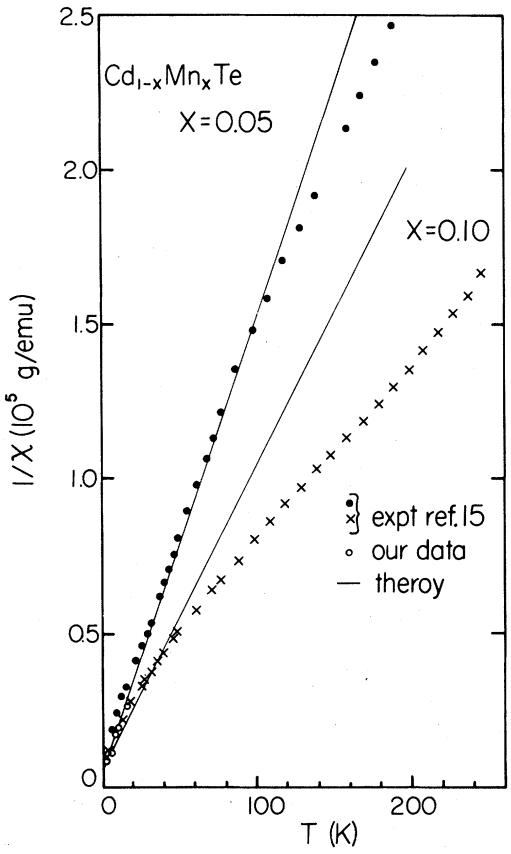

FIG. 13. Reciprocal susceptibility vs temperature for $x = 0.05$ and 0.10. The theoretical curves were calculated using the same distribution of clusters as for the specific heat. The number of singlets correspond to the 10-kG data (see Table III). Experimental points are from Ref. 15 and from our low-temperature measurements for $x = 0.10$.

theoretical susceptibility is lower than the experimental value. Because of the large J'_{NN} constant the effect is more pronounced at high temperatures.

VI. DISCUSSION AND CONCLUSIONS

Specific heat and magnetic susceptibility measurements performed in $Cd_{1-x}Mn_xTe$ in a wide range of Mn concentrations allow us to distinguish three ranges of x with different magnetic properties. For $x < 0.2$, a paramagnetic region occurs, for $0.2 \leq x \leq 0.60$ a spin-glass phase is observed, and the range $x < 0.70$ corresponds to an antiferromagnetic structure.

Theoretical analyses of experimental data show a nonstatistical distribution of singlets, pairs, and triplets in $Cd_{1-x}Mn_xTe$ crystals. The number of all types of clusters considered is larger than statistically predicted. However, for a small concentration of Mn ($x \leq 0.002$) the distribution of Mn atoms tends to be random.

Our theoretical model is applicable only to the paramagnetic region and does not consider clusters larger than triplets. We also neglect next-nearest-neighbor interactions, dipole-dipole interactions, and biquadratic terms.[35,36] However, our results, (at least up to $x = 0.05$), along with previously reported EPR data for $Cd_{1-x}Mn_xTe$ (Ref. 18) and susceptibility data for $Zn_xMn_{1-x}S$ (Ref. 13), indicate that good agreement between the theory and experiment can be obtained with linear terms alone. Comparing the experimental results of specific heat with theoretical curves, one notes some differences between the shape of both curves. The strongest deviations are observed for the composition $x = 0.10$ and 0.01 in zero magnetic field (Figs. 5 and 6). Some smaller deviations between theoretical curves and experimental results are also seen for $x = 0.002$, 0.10, and 0.05 samples. These deviations for $T < 3$ K exceed the limits of experimental error, which cannot be explained within the frame of our model. The best agreement for both low-temperature specific heat and magnetic susceptibility were obtained by assuming the exchange constant $J_{NN}/k = -0.55$ K.

However, using a molecular-field theory, the high-temperature susceptibility measurements for $x > 0.3$ (Ref. 19) give $J'_{NN}/k = -6$ K and the value of the susceptibility in the antiferromagnetic region for $x = 0.7$ gives $J'_{NN}/k = -4.3$ K. The high-temperature susceptibility measurements of $Zn_{1-x}Mn_xS$, referred to above, lead to values of $J/k = -8$ to -10 K.[13] It must be emphasized that the two exchange constants $J_{NN}/k = -0.55$ K and $J'_{NNN}/k = -4.3$ K are average values representing two *different* kinds of interactions present in the crystal. The J_{NN} exchange constant is connected with near-neighbor interactions in small noninteracting clusters, such as pairs or triangles, whereas J'_{NN} reflects the more collective interactions taking place in very large clusters. In general, even for pairs, the exchange integral in a fcc lattice is a nine-component tensor[37] and for larger clusters it is a higher order tensor. We treat the exchange constant as a scalar in both cases, i.e., in the cluster model and in the molecular-field theory, and in this sense the exchange constants are average values.

In the spin-glass phase, some differences were observed in the behavior of the susceptibility as compared to the case of metallic spin-glasses slightly above the transition temperature. The susceptibility is independent of past magnetic history for metallic spin-glasses in this region, but for these tellurium compounds it exhibits an irreversible behavior. This is probably related to the difference in the nature of the magnetic interaction. In the metallic spin-glass the interaction is long range, while in the insulating compound the short-range interaction between the clusters may allow clusters to freeze at different tem-

peratures.

The crystal structure of these compounds is a zinc-blende structure. This structure is favorable to the formation of a spin-glass phase due to the lattice frustration, since the magnetic sites form a fcc lattice. The existence of a next-nearest-neighbor interaction J_{NNN} between magnetic ions is expected to be much smaller than J_{NN}.[13] Therefore we conclude that the frustration mechanism is responsible for the spin-glass phase in these crystals.

The linear term in the specific heat at low temperatures, which has been previously observed in metallic spin-glasses, is found in our case for $x = 0.20$ and 0.30. In contrast, self-consistent field theory leads to $C \sim T^3$. Other existing theoretical approaches[16,38] seem to be inapplicable for the physical situations with which we are dealing, or predict results which differ from the experiment.[39] The specific heat in sample $x = 0.50$ calls for special attention. Susceptibility measurements show a cusp for $T = 12$ K, but no linear term is observed in the specific-heat experiment, i.e., in the region 0.5 to 10 K the specific heat can be described completely by a nuclear term and two cubic terms corresponding to spin-wave and lattice contributions. This is a nontypical behavior for a spin-glass. Neutron-diffraction investigations recently performed can throw additional light on this problem. These experiments show weak peaks corresponding to a short-range ordering at low (6 K) temperature, but not at 78 K and room temperature.[40] It is well known, however, that no peak in neutron diffraction is observed for a typical spin-glass phase. It is possible, therefore, that a mixed structure takes place in this material, where an infinite cluster (or a few very large clusters) corresponding to the spin-glass phase contains a number of well-ordered antiferromagnetic grains. The size and density of these grains are a function of x. The presence of well-ordered grains is probably connected with the spin-wave term which dominates the linear term characteristic of the spin-glass specific heat.

Our experiments, together with neutron-diffraction measurements, allow us to picture the evolution of magnetic interaction in $Cd_{1-x}Mn_xTe$ as a function of Mn concentration. For low values of x the system is paramagnetic, with the tendency to clustering that is stronger than statistically predicted. For $x \simeq 0.17$ clusters are large enough to produce a spin-glass phase due to the frustration of the lattice. For higher concentrations of Mn in the spin-glass structure, it is likely that finite antiferromagnetic grains appear, their size increasing with increasing concentration of Mn ions. The transition from the spin-glass to the antiferromagnetic phase probably requires some critical grain density which is also connected with their size. Assuming a finite size of grains, one can imagine the existence of percolation threshold between the grains, which leads to the spin-glass–antiferromagnet transition. This idea requires further evidence, especially through neutron-diffraction studies, in order to describe the type of antiferromagnetic ordering in these grains, as well as their size.

ACKNOWLEDGMENTS

The authors would like to thank Professor G. S. Grest and Professor J. K. Furdyna for critical reading of the manuscript, and also for their valuable comments and discussions during the course of this work. This research was supported by National Science Foundation MRL Grant No. DMR 77-23798.

---

*On leave from Institute of Physics, Polish Academy of Sciences, Warsaw, Poland.

[1]R. R. Galazka, in *Physics of Semiconductors 1978,* edited by B. L. H. Wilson, IOP Conf. Proc. No. 43 (IOP, Bristol and London, 1978), p. 133.

[2]B. Orlowski, Phys. Status Solidi (b) 95, K31 (1979).

[3]J. A. Gaj, R. R. Galazka, and M. Nawrocki, Solid State Commun. 23, 894 (1977).

[4]J. A. Gaj, R. Planel, and G. Fishman, Solid State Commun. 29, 435 (1978).

[5]K. Tanaka, M. Ishikane, M. Inoue, and H. Yagi, Jpn. J. Appl. Phys. 16, 783 (1977).

[6]J. A. Gaj, J. Ginter, and R. R. Galazka, Phys. Status Solidi (b) 89, 655 (1978).

[7]N. T. Khoi and J. A. Gaj, Phys. Status Solidi (b) 83, K133 (1977).

[8]L. De Seze, J. Phys. C 10, L353 (1977).

[9]G. Toulouse, Commun Phys. 2, 115 (1977).

[10]J. Villain, Z. Phys. B 33, 31 (1979).

[11]G. S. Grest and E. F. Gabl, Phys. Rev. Lett. 43, 1182 (1979).

[12]H. Maletta and W. Felsch, Phys. Rev. B 20, 1245 (1979).

[13]W. H. Brumage, C. R. Yager, and C. C. Lin, Phys. Rev. 133, A765 (1964).

[14]R. R. Galazka, S. Nagata, and P. H. Keesom, Bull. Am. Phys. Soc. 25, 177 (1980).

[15]R. A. Verhelst, R. W. Kline, A. M. de Graaf, and H. O. Hooper, Phys. Rev. B 11, 4427 (1975).

[16]M. W. Klein, Phys. Rev. B 14, 5008 (1976).

[17]V. Sondermann, J. Magn. Magn. Mater. 2, 216 (1976).

[18]M. F. Deigen, V. Ya. Zevin, V. M. Maevskii, I. V. Potykevich, and B. D. Shanina, Sov. Phys. Solid State 9, 773 (1967).

[19]Z. Wilamowski and R. R. Galazka, Phys. Status Solidi (in press).

[20]A. H. Dadeek, Ph.D. thesis (Rensselaer Polytechnic Institute, 1971) (unpublished).

[21]J. Bak, U. Debska, R. R. Galazka, G. Jasiolek, E. Mizera, and B. Bryza, Suppl. Acta Crystallogr. A 34, 245 (1978).

[22]R. E. Behringer, J. Chem. Phys. 29, 537 (1958).

[23]S. Nagata, R. R. Galazka, D. Mullin, H. Akbarzadeh, G.

D. Khattak, P. H. Keesom, and J. K. Furdyna, Phys. Rev. B 22 3331 (1980) (preceding paper).
[24]D. Mateika, J. Cryst. Growth 13/14, 698 (1972).
[25]K. Walther, Solid State Commun. 5, 399 (1967).
[26]G. M. Seidel and P. H. Keesom, Rev. Sci. Instrum. 29, 606 (1958).
[27]S. Nagata, P. H. Keesom, and H. R. Harrison, Phys. Rev. B 19, 1633 (1979).
[28]A. P. Rusakov, Yu. Kh. Vekilov, and A. E. Kadyshevich, Sov. Phys. Solid State 12, 2618 (1971); also J. A. Birch, J. Phys. C 8, 2043 (1975).
[29]B. Dreyfus, J. Souletie, R. Tournier, and L. Weil, C. R. Acad. Sci. 259, 4266 (1964).
[30]L. E. Wenger and P. H. Keesom, Phys. Rev. B 13, 4053 (1976).
[31]N. E. Phillips, Crit. Rev. Solid State Sci. 2, 467 (1971).
[32]R. G. Scurlock and W. N. R. Stevens, Proc. Phys. Soc. London 86, 331 (1965).
[33]H. Montgomery, Ann. Acad. Sci. Fenn. Ser. A6 210, 214 (1966).
[34]J. L. Tholence and R. Tournier, J. Phys. (Paris) 35, C4-299 (1974).
[35]P. W. Anderson, Phys. Rev. 115, 2 (1959); *Solid State Physics*, edited by F. Seitz and D. Turnbull (Academic, New York, 1963), Vol. 14, p. 99.
[36]E. A. Harris and J. Owen, Phys. Rev. Lett. 11, 9 (1963).
[37]J. Ginter, J. Kossut, and L. Swierkowski, Phys. Status Solidi (b) 96, 735 (1979).
[38]A. A. Abrikosov and S. I. Moukhin, J. Low Temp. Phys. 33, 207 (1978).
[39]S. E. Edwards and P. W. Anderson, J. Phys. F 5, 965 (1975).
[40]T. Giebultowicz, H. Kepa, and R. R. Galazka (unpublished).